HHS Public Access

Author manuscript

J Alzheimers Dis. Author manuscript; available in PMC 2016 January 01.

Published in final edited form as:

J Alzheimers Dis. 2015 ; 45(4): 1139–1148. doi:10.3233/JAD-142154.

Axonal Terminals Exposed to Amyloid-β May Not Lead to Pre-Synaptic Axonal Damage

Shu-Wei Sun[a,b,c,d,e,*], **Christopher Nishioka**[d], **Wessam Labib**[f], and **Hsiao-Fang Liang**[a]

[a]Basic Sciences, Schools of Medicine, Loma Linda University, Loma Linda, CA, USA

[b]Radiation Medicine, Schools of Medicine, Loma Linda University, Loma Linda, CA, USA

[c]Pharmaceutical Science, School of Pharmacy, Loma Linda University, Loma Linda, CA, USA

[d]Neuroscience, University of California in Riverside, Riverside, CA, USA

[e]Bioengineering, University of California in Riverside, Riverside, CA, USA

[f]Family Medicine, Loma Linda University Medical Center, Loma Linda, CA, USA

Abstract

Background—Synaptic deficits and neuronal loss are the major pathological manifestations of Alzheimer's disease. However, the link between the early synaptic loss and subsequent neurodegeneration is not entirely clear. Cell culture studies have shown that amyloid-β (Aβ) applied to axonal terminals can cause retrograde degeneration leading to the neuronal loss, but this process has not been demonstrated in live animals.

Objective—To test if Aβ applied to retinal ganglion cell axonal terminals can induce axonal damage in the optic nerve and optic tract in mice.

Methods—Aβ was injected into the terminal field of the optic tract, in the left lateral geniculate nucleus of wildtype C57BL/6 mice. Following the injection, monthly diffusion tensor imaging was performed. Three months after the injection, mice underwent visual evoked potential recordings, and then sacrificed for immunohistochemical examination.

Results—There were no significant changes seen with diffusion tensor imaging in the optic nerve and optic tract 3 months after the Aβ injection. The myelin and axons in these regions remained intact according to immunohistochemistry. The only significant changes observed in this study were delayed transduction and reduced amplitude of visual evoked potentials, although both Aβ and its reversed form caused similar changes.

Conclusion—Despite the published *in vitro* studies, there was no significant axonal damage in the optic nerve and optic tract after injecting Aβ onto retinal ganglion cell axonal terminals of wildtype C57BL/6 mice.

[*]Correspondence to: Shu-Wei (Richard) Sun, PhD, Basic Sciences, School of Medicine, Loma Linda University, Loma Linda, CA 92354, USA. Tel.: +1 909 558 7115; rsun@llu.edu.

Authors' disclosures available online (http://jalz.com/manuscript-disclosures/14-2154r1).

Keywords

Amyloid-β injection; diffusion tensor image; mouse; retinal ganglion cell; retrograde degeneration; visual evoked potential

INTRODUCTION

Alzheimer's disease (AD) is the leading cause of senior dementia. One in three seniors' die with dementia, and AD is the sixth leading cause of death in the United States. The initial symptoms of memory loss and cognitive decline have been associated with synaptic deficits caused by the toxic effects of amyloid-β (Aβ) [1–8]. During the course of AD, many regions of the brain lose substantial numbers of neurons. Compared to the initial synaptic deficits, loss of neurons may constitute a later, more irreversible damage to the nervous system. However, the mechanisms leading to neuronal loss in AD are still not fully understood.

In the nervous system, Aβ is produced from the proteolysis of amyloid-β protein precursor (Aβ PP) [9–11] and possibly released from axonal terminals into the extracellular space [12, 13]. To examine whether the axonal terminal associated Aβ can cause retrograde axonal degeneration, recent cell culture studies using microfluidic devices have demonstrated that selectively providing Aβ to axonal terminals not only reduce proximal synapses but also induce axonal fragmentation and neuronal apoptosis [14–16]. Aβ-induced retrograde axonal degeneration could be a possible mechanism of Aβ-induced neuronal loss in AD, but this phenomenon has not been examined *in vivo*. We recently investigated the white matter integrity in mice after Aβ intracerebroventricular injection. Two months after the injection, severe axonal and myelin damage was found in the optic nerves (ON) and optic tracts (OT) [17]. Because the neuronal bodies of the axons of ON and OT are retinal ganglion cells (RGC) located in the eye, the damage to the ON and OT were not likely due to direct effects of Aβ on the somata or dendrites, but possibly due to the vicinity of nerve fibers to the injected Aβ. Altogether, data supports the idea that Aβ may induce retrograde axonal degeneration, providing a possible mechanism of neuronal loss in AD.

RGCs, whose cell bodies are within the eye, while their axons form the ON and OT in the brain, provide a novel *in vivo* model to allow selective exposure of axonal terminals to Aβ. In this study, we injected Aβ specifically into the OT terminal field located in the lateral geniculate nucleus (LGN). To evaluate the changes within the ON and OT longitudinally, diffusion tensor imaging (DTI) was used to track the degeneration process monthly for 3 months after the injection [17–21]. DTI is a non-invasive magnetic resonance imaging (MRI) modality, which quantifies molecular water diffusion in 3-dimensional space. Because water diffusion is restrained by cell membranes and organelles, DTI derived indices can reveal tissue microstructural changes, which can serve as *in vivo* surrogate markers for neural damage [20–25]. In white matter fiber tracts, water diffuses more readily along the fibers then those across the fibers. The difference of diffusion along various directions can be quantified as diffusion anisotropy, which includes relative anisotropy (RA) and fractional anisotropy (FA). White matter disruption usually leads to a decrease of diffusion anisotropy. Thus, diffusion anisotropy has been used as a non-invasive marker of white matter damage.

In addition, from DTI, one can also derive the trace of diffusion tensor (Tr), which quantifies the average water diffusion in all directions, axial diffusivity ($\lambda_{\parallel}$), the diffusion along the axis of fiber bundles, and radial diffusivity ($\lambda_{\perp}$), the diffusion across the fiber bundles. We have previously demonstrated that $\lambda_{\parallel}$ and $\lambda_{\perp}$ are sensitive to the axonal and myelin damage respectively in mouse ON and OT [21].

At the end of the time course, visual evoked potentials (VEPs) were recorded to examine the electrophysiological condition of the visual system of each animal. Animals were then sacrificed for tissue examination by immunohistochemistry. Antibodies against neurofilament and myelin basic protein were utilized to assess the integrity of axon and myelin of nerves affected by Aβ [26, 27].

MATERIALS AND METHODS

All experimental procedures were in accordance with National Institutes of Health guidelines and were approved by the Institutional Animal Care and Use Committee of the Loma Linda University.

Injection

Human $A\beta_{1–42}$ (A9810, Sigma Aldrich, USA) or the reverse peptide (rAβ, SCP0048, Sigma Aldrich, USA) were dissolved in sterile saline and incubated at 37°C for 72 h [28–30]. This process allowed Aβ to form aggregates before being injected into the animals. Twelve female C57BL/6 mice at 12-weeks old were anesthetized by 1.5% isoflurane/oxygen using an isoflurane vaporizer (VetEquip, Pleasanton, CA). The body temperature was maintained using an electric heating pad. Mice were placed in a stereotactic apparatus. Fur above the incision site was shaved and skin was cleaned with iodine. Aβ 4 nmole/3 μl (n = 8) or 10 nmole/3 μl (n = 5), or rAβ 4 nmole/3 μl (n = 5) was injected 0.1μl/min into the left OT terminal area located in LGN (coordinates: posterior 2.0mm from the bregma, lateral 2.0mm left lateral to midline, and 2–2.5mm ventral to the cortical surface), using a 10-μl Hamilton syringe [28–30]. The needle was kept in the injection site for 5 min and then withdrawn 0.5mm every 5 min until completely removed from the skull.

Imaging procedure

Before injection and monthly after injection, mice were examined with DTI. Mice were anesthetized with a mixture of oxygen and isoflurane. Core body temperature was maintained at 37.0 ± 0.5°C using warm water circulating in a pad. Mice were placed in a holder to immobilize the head. A 7-cm inner volume coil was used as a transmitter coil and a 1.5-cm inner diameter surface coil was used as a receiver to collect data in a Bruker 4.7T BioSpec small animal MRI instrument. Images with slice thickness 0.5 mm, field of view of 2 cm × 2 cm and matrix 128 × 128 (zero filling to 256 × 256) were collected to cover the visual system from the eye to superior colliculus. Spin-echo DTI was performed with TR 3 s, TE 29 ms, duration between a diffusion gradient pair (Δ) = 20 ms, diffusion gradient duration (δ) = 3 ms, and six-direction diffusion scheme with b-values of 0 and 0.85 ms/μm^2. Using software written in Matlab (MathWorks, Natick, MA, USA), the eigenvalues (λ_1, λ_2,

and λ_3) derived from diffusion tensor were used to calculate $\lambda_{\|}$, $\lambda_{\perp}$, RA, and Tr defined by the following equations:

$$\mathrm{Tr}=\lambda_1+\lambda_2+\lambda_3 \quad (1)$$

$$\lambda_{\|}=\lambda_1 \quad (2)$$

$$\lambda_{\perp}=0.5\times(\lambda_2+\lambda_3) \quad (3)$$

$$\mathrm{RA}=\frac{\sqrt{(\lambda_1-\mathrm{Tr}/3)^2+(\lambda_2-\mathrm{Tr}/3)^2+(\lambda_3-\mathrm{Tr}/3)^2}}{\sqrt{3}(\mathrm{Tr}/3)} \quad (4)$$

Regions of interest (ROI) were selected in the ON and OT referenced to the mouse brain atlas [31]. Data were presented as mean ± standard deviation. Paired *t*-tests were used to compare DTI indices between the ipsilateral and contralateral sides for each ROI. Repeated measures analysis of variance (ANOVA)was carried out to compare the time course of each measurement between Aβ-treated and control mice. *P*-values were considered to be statistically significant at $\alpha < 0.05$. All statistical analyses were conducted with Matlab (MathWorks, Natick, MA, USA).

Visual evoked potential

Core body temperature was maintained at 37.0 ± 0.5°C using a heating pad. To minimize discomfort, Lidocaine was applied to all incision sites and soft tissue pressure points. A midline incision was made to expose the skull. Two small holes were drilled and silver wires were placed over the visual cortex (0.5 mm anterior and 2.5 mm lateral to the Lambda point) and cerebellum (1.5 mm posterior to Lambda) for recording and reference, respectively [32]. After dark adaption for 10 min, light stimulation was produced by a LED light source (Radioshack, Fort Worth, TX), at frequency of 0.2 Hz with a duration of 5ms [33]. Field potentials were recorded using a CyberAmp380 amplifier (Molecular Devices, Sunnyvale, CA) and a Digidata1440A interface (Molecular Devices, Sunnyvale, CA), with a sampling rate of 20 KHz and a bandpass filter of 0.1–300 Hz, controlled by Clampex 10.2 (Molecular Devices, Sunnyvale, CA). Averaged data from 100 continuous traces was used to calculated implicit time and amplitude of major negative component for each mouse.

Immunohistochemistry examination

At 3 months after Aβ treatment, animals were intracardially perfused with4%paraformaldehyde in PBS.A 4-mm-thick coronal section (−1 to +3mm of bregma) was obtained from each brain and embedded in paraffin. Brain tissue slices, 3μm thickness, matching the MRI imaging sections, were cut and deparaffinized in xylene for immunohistochemical examinations. The integrity of axons was evaluated using a primary antibody against phosphorylated neurofilament (SMI-31, 1:1000; Sternberger Monoclonals, Lutherville, Maryland), and myelin integrity was assessed with a primary antibody against

myelin basic protein (MBP, 1:250; Zymed Laboratories Inc., South San Francisco, CA) at 4°C overnight [34]. Following a 15-min wash in PBS, sections were incubated in fluorescent secondary antibodies for 1 h at room temperature (1:200, Goat anti-mouse conjugated to Texas red for SMI-31, 1:200, Goat anti-rabbit conjugated to green for MBP; Molecular Probes). Immunohistochemistry of glial fibrillary acidic protein (GFAP, 1:1000, Cell Signaling) was also performed. Histological sections were examined using an Olympus Fluoview confocal microscope equipped with a 60× oil objective. The red SMI-31 positive staining, representing the normal axons, was captured. Axons were counted through the central 70 × 70μm^2 regions. The counts per 100 μm^2 were presented as mean ± standard deviation.

RESULTS

Representative DTI maps, including $\lambda_{\parallel}$, $\lambda_{\perp}$, RA, and TR, of mouse brains from the Aβ-treated and control mice are shown in Fig. 1. White matter tracts, including ON and OT, can be easily identified. DTI maps of Aβ-treated mice appear similar to those acquired from the control mice. Quantitative analysis, including $\lambda_{\parallel}$, $\lambda_{\perp}$, RA, and TR from ON and OT are summarized in Fig. 2. The time course of DTI indices show small fluctuations, but these changes are not statistically significant. Increasing the dosage of Aβ from 4 to 10 nmole did not lead to significant differences in DTI either; DTI of ON and OT from both groups are statistically indistinguishable from control mice.

Immunohistochemistry using SMI-31 and MBP was performed to examine the integrity of axons and myelin of ON and OT in 3 months after Aβ treatments (Fig. 3). The Aβ-treated nerves did not show significant damage compared to control nerves. We also stained for GFAP to examine potential astrocytic reaction in these nerves. Again, astrocyte morphology appeared normal in ON and OT of Aβ-treated mice (Fig. 4).

The only significant changes in the Aβ-treated mice were observed in the recorded VEP (Fig. 5), which quantifies the nerve transduction from retina to visual cortex. Three months after the injection of 4 nmole Aβ, Aβ-affected visual pathways showed a significant 40–50% reduction of VEP amplitude; in contrast, the VEPs from contralateral eyes of the same mice remained normal. Similar effects were found in mice after a 10 nmole Aβ injection, which showed a significant 60–70% reduction of the VEP amplitude and a significant 16–26% increase of the VEP latency in the Aβ-affected pathway, with normal VEPs recorded from contralateral eyes. Mice injected with reverse Aβ peptide (rAβ, 4 nmole) also had changes in VEP. The rAβ-affected eyes showed a significant 56–67% reduction of the VEP amplitude and a significant 10–16% increase of the VEP latency, and the contralateral eyes showed normal VEPs recorded.

DISCUSSION

In this study, we examined whether Aβ can induce retrograde degeneration in live mice. We took the advantage of the unique anatomical features of RGCs to selectively expose their axon terminals to Aβ. *In vivo* DTI and postmortem immunohistological examinations confirmed that the axons of RGCs, which form ON and OT in the brain, remained intact 3

months after Aβ injection. However, the VEP examinations showed ~50%reduction of amplitude and ~20%delay in the Aβ-affected visual pathways compared to the controls. These findings indicate that the injected Aβ did impede flow of visual information from the retina to visual cortex, though it did not cause noticeable RGC degeneration.

Although the manifestation of AD is likely due to many factors, Aβ, a key component of amyloid plaques, is important in the pathogenesis of AD [2]. Aβ is produced from the cleavage of Aβ PP [35], which is transported centrifugally along axons from somata to the axonal terminals [13]. Thus, it has been speculated that Aβ released from axonal terminals may have detrimental effects on its cell of origin. In the brains of AD patients, a reduction of basal forebrain cholinergic neurons has been commonly reported [36]. However, their cell bodies are located in nuclei physically remote from areas of preferential Aβ accumulation [37, 38], indicating possible Aβ-induced retrograde degeneration [39]. Results from *in vitro* experiments support this idea [16, 40, 41]. Novel microfabrication and microfluidic technologies have enabled the development of cell culture devices with multiple-compartmental chambers connected with micron-size grooves. Neurons plated in one compartment can grow axons across the compartments while maintaining fluidic isolation [16]. Using these devices, studies have found that selective exposure of axons and axon terminals to Aβ can cause axonal destruction, which leads to nuclear apoptosis [14–16]. In sum, evidence suggests that exposing axon terminals to Aβ may play a critical role in initiating retrograde neurodegeneration in patients with AD.

We have previously investigated white matter integrity in mice after an Aβ injection into the lateral ventricle [17]. Two months after the injection, the OTs, which are located adjacent to the Aβ-injected ventricle, showed a significant 83% increase in $\lambda_{\perp}$ and a significant 31% decrease in RA of measurements from *in vivo* DTI. Similar damage extended to ON of the same mice. This damage was confirmed by the immunohistochemistry showing significant 30–40% loss of axons and myelin. Given that the axons of ON and OT have their cell bodies located in the eyes, the data supported the idea that Aβ could precipitate axonal degeneration without affecting soma or dendrites first. However, the exact route of Aβ exposure necessary to trigger the damage is unclear. In the present study, exposing OT axonal terminal areas to Aβ did not cause significant damage to ON and OT. We suspect that Aβ intracerebroventricular injection may cause more profound effects on mice perhaps by triggering immune responses and enhancing the cellular stress, leading to a larger degree of damage compared to focal injection of Aβ in this study. It is also possible that the Aβ intracerebroventricular injection directly affected myelin and axons of the visual pathway, in addition to axonal terminals as in this study [42–44]. Further investigations are needed to better understand the mechanisms responsible for retrograde axonal degeneration in AD.

A unique feature of the present study is that both structural and functional assessments were taken to evaluate the visual system in mice affected by Aβ. DTI provided high resolution measurements for microstructural changes in ON and OT. Meanwhile, VEP provided functional assessments for the visual system. We found no evidence of structural change based on DTI, but all animals suffered from functional declines based on VEP. Structural and functional assessments offer complementary information about the condition of the nervous system. In most cases, structural imaging provides better spatial information to

characterize location of damage. However, as shown in this study, the functional declines can be significant even if there are no detectable changes by structural imaging. Both functional and structural examinations need to be taken into account to provide a better evaluation of the nervous system.

Visual problems are commonly observed in AD patients. Low-level measures of visual ability in tests of stereo acuity, color discrimination, contrast sensitivity, visual processing speed, and visual field coverage are worse in AD patients, compared to the similarly aged controls [45–55]. Although visual problems are not usually considered as a disease hallmark of AD, the visual deficits have been found to correlate with the severity of dementia [56], suggesting that visual declines and dementia may share the same pathogenesis in AD. Assessing retinal degeneration in patients may serve as an important biomarker in improving the diagnosis and therapeutic outlook for AD patients [57, 58].

The size of LGN is relatively substantial, with its middle transactional size similar to a lateral ventricle [31]. Thus, micro injection into the LGN was not technically challenging, compared to the ventricular injection, which is a common procedure in a neuroscience lab. It would be ideal in this study if the needle traces could be examined in all mice to confirm the correct location of the injection. When examining these animals using MRI and postmortem histology in this study, however, we were only able to characterize partial but not the complete needle traces. Since the MRI and histology were performed months after injection, we suspect that the brain tissue separated by the needle may have been partially repaired. Although the misallocation of an injection site could be a concern, deteriorated VEPs were consistently recorded from the injected mice suggesting that the injection affected the visual system in all mice. Altogether, the data support that the injection successfully delivered Aβ to the LGN, which caused significant delay in VEPs but did not lead to detectable damage in ON and OT.

It is not clear why both Aβ and its reversed form (rAβ) altered VEPs. rAβ injection was used as a control group because it was assumed to be inactive with same molecular weight of Aβ. However, the exact biological effects of rAβ are not known. Despite its reversed form, rAβ may contain fragments which are toxic to synapses, and possibly damage neurons [59, 60]. Based on the studies from literature, it is not uncommon for reversed or scrambled forms of Aβ to be excluded from control groups in studies using Aβ. rAβ may have biological effects which warrant further investigations.

It is worth to note that prior studies have demonstrated that the monomeric Aβ is less toxic than its oligomeric or fibrillar forms [61]. Thus, before the injection into animals, Aβ was incubated at 37°C for 72 h to form aggregates [28–30]. These aggregates can be detected microscopically using Congo red staining. The injected aggregates may be neurotoxic due to several features: 1) They can serve as a reservoir to gradually release toxic Aβ oligomers to injure the brain [61]; 2) The released aggregates may serve as seeds to spread the damage to larger brain areas [62]; and 3) Aggregates may induce microglial activation and precipitate neuro-inflammatory damage [63]. Altogether, the incubation process is a critical step to vender strong Aβ toxic effects in the animals [28–30].

In conclusion, this study examined whether exposing OT axonal terminals to Aβ could cause axonal damage in the ON and OT. Three months after the Aβ treatment, we did not find significant damage to the ON and OT. The only deficits we observed were the alteration of recorded VEPs. Our data suggest that a single dose of Aβ (4 nmole and 10 nmole) can alter neural conduction but not cause significant retrograde axonal degeneration in the visual pathway of live animals.

ACKNOWLEDGMENTS

This study was partly supported by NIH 1R01NS062830. We especially thank Dr. Wei-Xing Shi for the insightful discussion and his generosity providing facilities for VEP recording.

REFERENCES

1. Selkoe DJ. Preventing Alzheimer's disease. Science. 2012; 337:1488–1492. [PubMed: 22997326]
2. Selkoe DJ. Resolving controversies on the path to Alzheimer's therapeutics. Nat Med. 2011; 17:1060–1065. [PubMed: 21900936]
3. Holtzman DM, Mandelkow E, Selkoe DJ. Alzheimer disease in 2020. Cold Spring Harb Perspect Med. 2012; 2 pii: a011585.
4. Kamenetz F, Tomita T, Hsieh H, Seabrook G, Borchelt D, Iwatsubo T, Sisodia S, Malinow R. APP processing and synaptic function. Neuron. 2003; 37:925–937. [PubMed: 12670422]
5. Wei W, Nguyen LN, Kessels HW, Hagiwara H, Sisodia S, Malinow R. Amyloid beta from axons and dendrites reduces local spine number and plasticity. Nat Neurosci. 2010; 13:190–196. [PubMed: 20037574]
6. Wang Z, Wang B, Yang L, Guo Q, Aithmitti N, Songyang Z, Zheng H. Presynaptic and postsynaptic interaction of the amyloid precursor protein promotes peripheral and central synaptogenesis. J Neurosci. 2009; 29:10788–10801. [PubMed: 19726636]
7. Hardy JA, Higgins GA. Alzheimer's disease: The amyloid cascade hypothesis. Science. 1992; 256:184–185. [PubMed: 1566067]
8. Terry RD, Masliah E, Salmon DP, Butters N, DeTeresa R, Hill R, Hansen LA, Katzman R. Physical basis of cognitive alterations in Alzheimer's disease: Synapse loss is the major correlate of cognitive impairment. Ann Neurol. 1991; 30:572–580. [PubMed: 1789684]
9. Kang J, Lemaire HG, Unterbeck A, Salbaum JM, Masters CL, Grzeschik KH, Multhaup G, Beyreuther K, Muller-Hill B. The precursor of Alzheimer's disease amyloid A4 protein resembles a cell-surface receptor. Nature. 1987; 325:733–736. [PubMed: 2881207]
10. Zimmermann K, Herget T, Salbaum JM, Schubert W, Hilbich C, Cramer M, Masters CL, Multhaup G, Kang J, Lemaire HG, et al. Localization of the putative precursor of Alzheimer's disease-specific amyloid at nuclear envelopes of adult human muscle. EMBO J. 1988; 7:367–372. [PubMed: 2896589]
11. Selkoe DJ. Amyloid beta-protein and the genetics of Alzheimer's disease. J Biol Chem. 1996; 271:18295–18298. [PubMed: 8756120]
12. Cirrito JR, Yamada KA, Finn MB, Sloviter RS, Bales KR, May PC, Schoepp DD, Paul SM, Mennerick S, Holtzman DM. Synaptic activity regulates interstitial fluid amyloidbeta levels *in vivo* . Neuron. 2005; 48:913–922. [PubMed: 16364896]
13. Lee EB, Zhang B, Liu K, Greenbaum EA, Doms RW, Trojanowski JQ, Lee VM. BACE overexpression alters the subcellular processing of APP and inhibits Abeta deposition *in vivo* . J Cell Biol. 2005; 168:291–302. [PubMed: 15642747]
14. Song MS, Saavedra L, de Chaves EI. Apoptosis is secondary to non-apoptotic axonal degeneration in neurons exposed to Abeta in distal axons. Neurobiol Aging. 2006; 27:1224–1238. [PubMed: 16122841]
15. Annweiler C, Brugg B, Peyrin JM, Bartha R, Beauchet O. Combination of memantine and vitamin D prevents axon degeneration induced by amyloid-beta and glutamate. Neurobiol Aging. 2014; 35:331–335. [PubMed: 24011542]

16. Taylor AM, Rhee SW, Tu CH, Cribbs DH, Cotman CW, Jeon NL. Microfluidic Multicompartment Device for Neuroscience Research. Langmuir. 2003; 19:1551–1556. [PubMed: 20725530]
17. Sun SW, Liang HF, Mei J, Xu D, Shi WX. *In vivo* diffusion tensor imaging of amyloid-beta-induced white matter damage in mice. J Alzheimers Dis. 2014; 38:93–101. [PubMed: 24077431]
18. Song SK, Kim JH, Lin SJ, Brendza RP, Holtzman DM. Diffusion tensor imaging detects age-dependent white matter changes in a transgenic mouse model with amyloid deposition. Neurobiol Dis. 2004; 15:640–647. [PubMed: 15056472]
19. Sun SW, Song SK, Harms MP, Lin SJ, Holtzman DM, Merchant KM, Kotyk JJ. Detection of age-dependent brain injury in a mouse model of brain amyloidosis associated with Alzheimer's disease using magnetic resonance diffusion tensor imaging. Exp Neurol. 2005; 191:77–85. [PubMed: 15589514]
20. Song SK, Sun SW, Ju WK, Lin SJ, Cross AH, Neufeld AH. Diffusion tensor imaging detects and differentiates axon and myelin degeneration in mouse optic nerve after retinal ischemia. Neuroimage. 2003; 20:1714–1722. [PubMed: 14642481]
21. Sun SW, Liang HF, Cross AH, Song SK. Evolving Wallerian degeneration after transient retinal ischemia in mice characterized by diffusion tensor imaging. Neuroimage. 2008; 40:1–10. [PubMed: 18187343]
22. Basser PJ, Jones DK. Diffusion-tensor MRI: Theory, experimental design and data analysis - a technical review. NMR Biomed. 2002; 15:456–467. [PubMed: 12489095]
23. Basser PJ. New histological and physiological stains derived from diffusion-tensor MR images. Ann N Y Acad Sci. 1997; 820:123–138. [PubMed: 9237452]
24. Basser PJ, Pierpaoli C. Microstructural and physiological features of tissues elucidated by quantitative-diffusion-tensor MRI. J Magn Reson B. 1996; 111:209–219. [PubMed: 8661285]
25. Basser PJ, Mattiello J, LeBihan D. MR diffusion tensor spectroscopy and imaging. Biophys J. 1994; 66:259–267. [PubMed: 8130344]
26. Sun SW, Liang HF, Schmidt RE, Cross AH, Song SK. Selective vulnerability of cerebral white matter in a murine model of multiple sclerosis detected using diffusion tensor imaging. Neurobiol Dis. 2007; 28:30–38. [PubMed: 17683944]
27. Sun SW, Liang HF, Xie M, Oyoyo U, Lee A. Fixation, not death, reduces sensitivity of DTI in detecting optic nerve damage. Neuroimage. 2009; 44:611–619. [PubMed: 19027864]
28. Mizoguchi H, Takuma K, Fukuzaki E, Ibi D, Someya E, Akazawa KH, Alkam T, Tsunekawa H, Mouri A, Noda Y, Nabeshima T, Yamada K. Matrix metalloprotease-9 inhibition improves amyloid beta-mediated cognitive impairment and neurotoxicity in mice. J Pharmacol Exp Ther. 2009; 331:14–22. [PubMed: 19587312]
29. Walsh DT, Bresciani L, Saunders D, Manca MF, Jen A, Gentleman SM, Jen LS. Amyloid beta peptide causes chronic glial cell activation and neuro-degeneration after intravitreal injection. Neuropathol Appl Neurobiol. 2005; 31:491–502. [PubMed: 16150120]
30. Walsh DT, Montero RM, Bresciani LG, Jen AY, Leclercq PD, Saunders D, A N, Gbadamoshi EL-A, Gentleman L, Jen SM, L S. Amyloid-beta peptide is toxic to neurons *in vivo* via indirect mechanisms. Neurobiol Dis. 2002; 10:20–27. [PubMed: 12079400]
31. Franklin, KB.; Paxinos, G. The Mouse Brain in Stereotaxic Coordinates. San Diego: Academic Press; 1997.
32. Porciatti V, Pizzorusso T, Maffei L. The visual physiology of the wild type mouse determined with pattern VEPs. Vision Res. 1999; 39:3071–3081. [PubMed: 10664805]
33. Peachey NS, Ball SL. Electrophysiological analysis of visual function in mutant mice. Doc Ophthalmol. 2003; 107:13–36. [PubMed: 12906119]
34. Sun SW, Liang HF, Trinkaus K, Cross AH, Armstrong RC, Song SK. Noninvasive detection of cuprizone induced axonal damage and demyelination in the mouse corpus callosum. Magn Reson Med. 2006; 55:302–308. [PubMed: 16408263]
35. Selkoe DJ. Alzheimer's disease: Genes, proteins, and therapy. Physiol Rev. 2001; 81:741–766. [PubMed: 11274343]
36. Auld DS, Kornecook TJ, Bastianetto S, Quirion R. Alzheimer's disease and the basal forebrain cholinergic system: Relations to beta-amyloid peptides, cognition, and treatment strategies. Prog Neurobiol. 2002; 68:209–245. [PubMed: 12450488]

37. Jacobs RW, Duong T, Scheibel AB. Immunohistochemical analysis of the basal forebrain in Alzheimer's disease. Mol Chem Neuropathol. 1992; 17:1–20. [PubMed: 1388447]
38. D'Andrea MR, Nagele RG, Wang HY, Peterson PA, Lee DH. Evidence that neurones accumulating amyloid can undergo lysis to form amyloid plaques in Alzheimer's disease. Histopathology. 2001; 38:120–134. [PubMed: 11207825]
39. Harkany T, Penke B, Luiten PG. beta-Amyloid excitotoxicity in rat magnocellular nucleus basalis. Effect of cortical deafferentation on cerebral blood flowregulation and implications for Alzheimer's disease. AnnNY Acad Sci. 2000; 903:374–386.
40. Pigino G, Morfini G, Atagi Y, Deshpande A, Yu C, Jungbauer L, LaDu M, Busciglio J, Brady S. Disruption of fast axonal transport is a pathogenic mechanism for intraneuronal amyloid beta. Proc Natl Acad Sci U S A. 2009; 106:5907–5912. [PubMed: 19321417]
41. Moreno H, Yu E, Pigino G, Hernandez AI, Kim N, Moreira JE, Sugimori M, Llinas RR. Synaptic transmission block by presynaptic injection of oligomeric amyloid beta. Proc Natl Acad Sci U S A. 2009; 106:5901–5906. [PubMed: 19304802]
42. Wolter JR. The centrifugal nerves in the human optic tract, chiasm, optic nerve, andretina. Trans Am Ophthalmol Soc. 1965; 63:678–707. [PubMed: 5859798]
43. Cowey A, Stoerig P. The neurobiology of blindsight. Trends Neurosci. 1991; 14:140–145. [PubMed: 1710851]
44. Morin LP. The circadian visual system. Brain Res Brain Res Rev. 1994; 19:102–127. [PubMed: 7909471]
45. Cronin-Golomb A, Corkin S, Rizzo JF, Cohen J, Growdon JH, Banks KS. Visual dysfunction in Alzheimer's disease: Relation to normal aging. Ann Neurol. 1991; 29:41–52. [PubMed: 1996878]
46. Trick GL, Trick LR, Morris P, Wolf M. Visual field loss in senile dementia of the Alzheimer's type. Neurology. 1995; 45:68–74. [PubMed: 7824139]
47. Tsai CS, Ritch R, Schwartz B, Lee SS, Miller NR, Chi T, Hsieh FY. Optic nerve head and nerve fiber layer in Alzheimer's disease. Arch Ophthalmol. 1991; 109:199–204. [PubMed: 1993028]
48. Baker DR, Mendez MF, Townsend JC, Ilsen PF, Bright DC. Optometric management of patients with Alzheimer's disease. J Am Optom Assoc. 1997; 68:483–494. [PubMed: 9279048]
49. Hinton DR, Sadun AA, Blanks JC, Miller CA. Opticnerve degeneration in Alzheimer's disease. N Engl J Med. 1986; 315:485–487. [PubMed: 3736630]
50. Sadun AA, Borchert M, DeVita E, Hinton DR, Bassi CJ. Assessment of visual impairment in patients with Alzheimer's disease. Am J Ophthalmol. 1987; 104:113–120. [PubMed: 3618708]
51. Blanks JC, Schmidt SY, Torigoe Y, Porrello KV, Hinton DR, Blanks RH. Retinal pathology in Alzheimer's disease. II. Regional neuron loss and glial changes in GCL. Neurobiol Aging. 1996; 17:385–395. [PubMed: 8725900]
52. Blanks JC, Torigoe Y, Hinton DR, Blanks RH. Retinal degeneration in the macula of patients with Alzheimer's disease. Ann N Y Acad Sci. 1991; 640:44–46. [PubMed: 1776758]
53. Blanks JC, Torigoe Y, Hinton DR, Blanks RH. Retinal pathology in Alzheimer's disease. I. Ganglion cell loss in foveal/parafoveal retina. Neurobiol Aging. 1996; 17:377–384. [PubMed: 8725899]
54. Hedges TR 3rd, Perez Galves R, Speigelman D, Barbas NR, Peli E, Yardley CJ. Retinal nerve fiber layer abnormalities in Alzheimer's disease. Acta Ophthalmol Scand. 1996; 74:271–275. [PubMed: 8828725]
55. Paquet C, Boissonnot M, Roger F, Dighiero P, Gil R, Hugon J. Abnormal retinal thickness in patients with mild cognitive impairment and Alzheimer's disease. Neurosci Lett. 2007; 420:97–99. [PubMed: 17543991]
56. Mendola JD, Cronin-Golomb A, Corkin S, Growdon JH. Prevalence of visual deficits in Alzheimer's disease. Optom Vis Sci. 1995; 72:155–167. [PubMed: 7609938]
57. Koronyo Y, Salumbides BC, Black KL, Koronyo-Hamaoui M. Alzheimer's disease in the retina: Imaging retinal abeta plaques for early diagnosis and therapy assessment. Neurodegener Dis. 2012; 10:285–293. [PubMed: 22343730]
58. Koronyo-Hamaoui M, Koronyo Y, Ljubimov AV, Miller CA, Ko MK, Black KL, Schwartz M, Farkas DL. Identification of amyloid plaques in retinas from Alzheimer's patients and noninvasive

in vivo optical imaging of retinal plaques in a mouse model. Neuroimage. 2011; 54(Suppl 1):S204–S217. [PubMed: 20550967]

59. Maurice T, Lockhart BP, Su TP, Privat A. Reversion of beta 25–35-amyloid peptide-induced amnesia by NMDA receptor-associated glycine site agonists. Brain Res. 1996; 731:249–253. [PubMed: 8883881]
60. Maurice T, Lockhart BP, Privat A. Amnesia induced in mice by centrally administered beta-amyloid peptides involves cholinergic dysfunction. Brain Res. 1996; 706:181–193. [PubMed: 8822355]
61. Haass C, Selkoe DJ. Soluble protein oligomers in neurodegeneration: Lessons from the Alzheimer's amyloid beta-peptide. Nat Rev Mol Cell Biol. 2007; 8:101–112. [PubMed: 17245412]
62. Walker LC, Diamond MI, Duff KE, Hyman BT. Mechanisms of protein seeding in neurodegenerative diseases. JAMA Neurol. 2013; 70:304–310. [PubMed: 23599928]
63. Griffin WS. Inflammation and neurodegenerative diseases. Am J Clin Nutr. 2006; 83:470S–474S. [PubMed: 16470015]

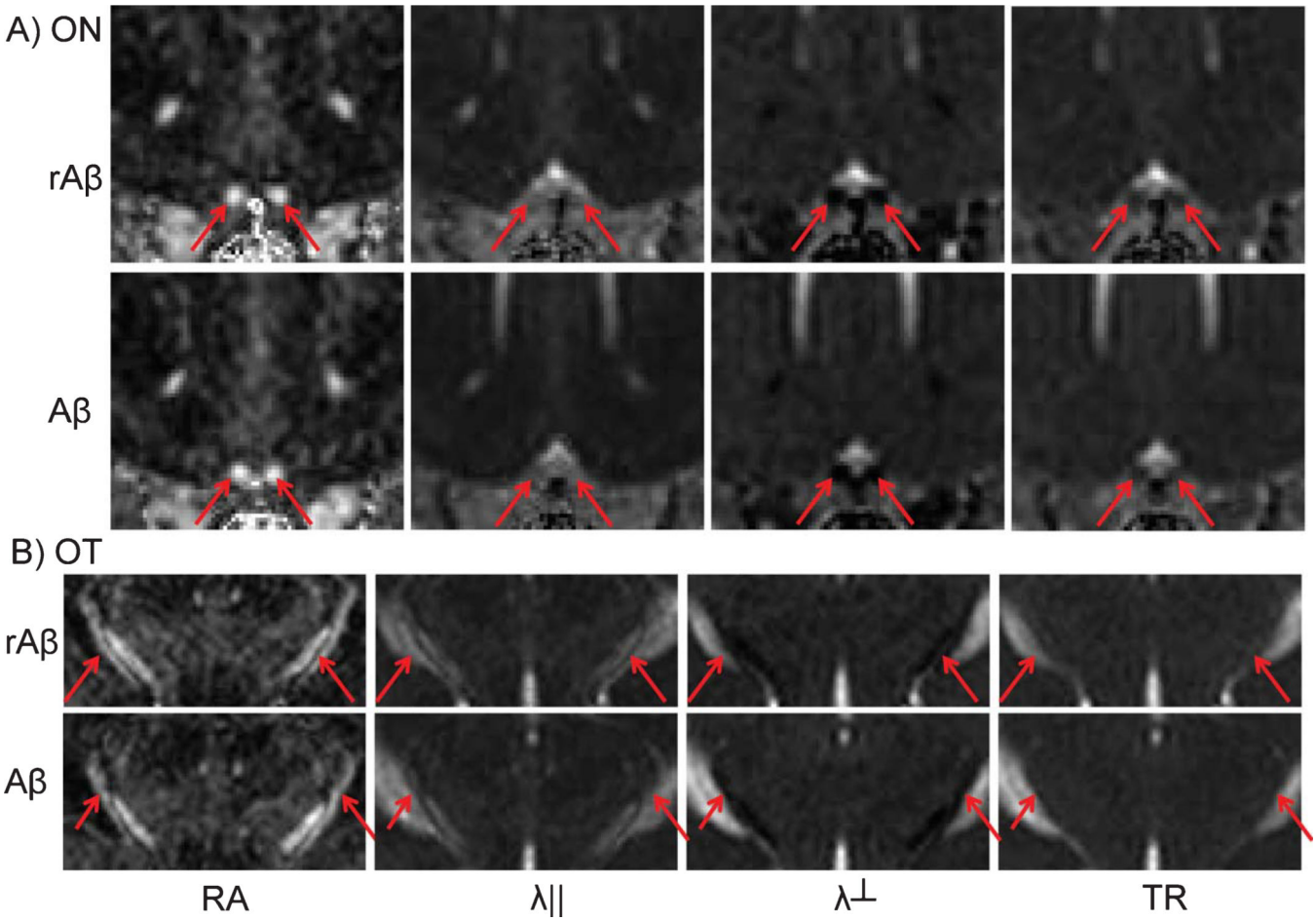

Fig. 1.

DTI maps of control and Aβ-treated mice. Representative DTI of mice 3 months after Aβ showed images similar to those acquired from mice 3 months after rAβ injection. The arrows indicate the optic nerves and tracts on RA, $\lambda_{||}$, $\lambda_{\perp}$, and TR maps.

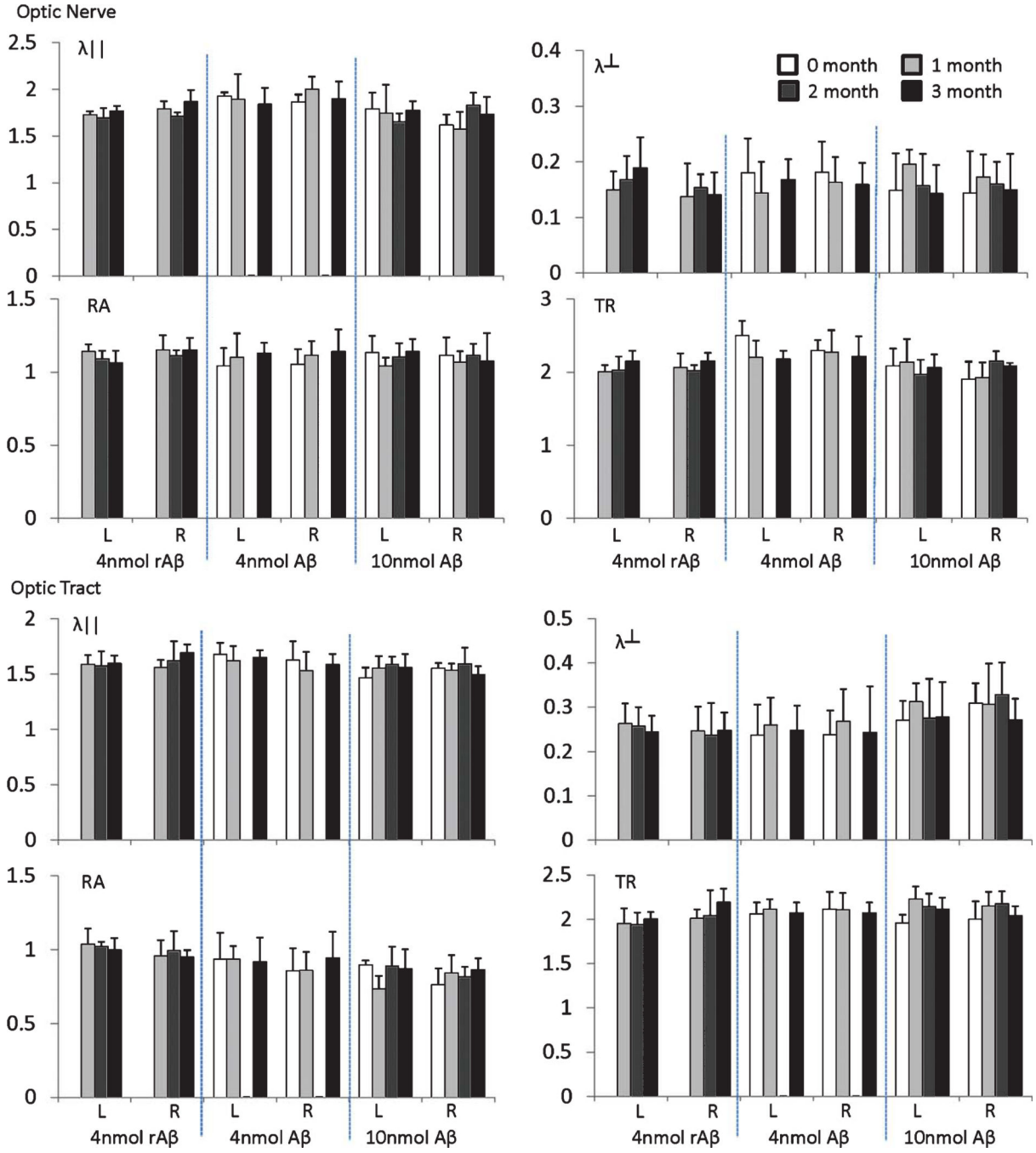

Fig. 2.

DTI measurements of the optic nerves and tracts after Aβ (4 n or 10 n mole) and rAβ injection in the left OT axonal terminals. The L and R indicate the left and right side of the ON and OT, respectively. The unit for $\lambda\|$, $\lambda_{\perp}$, and TR is $\mu m^2/ms$. RA is dimensionless. There was no significant change compared to the normal nerves.

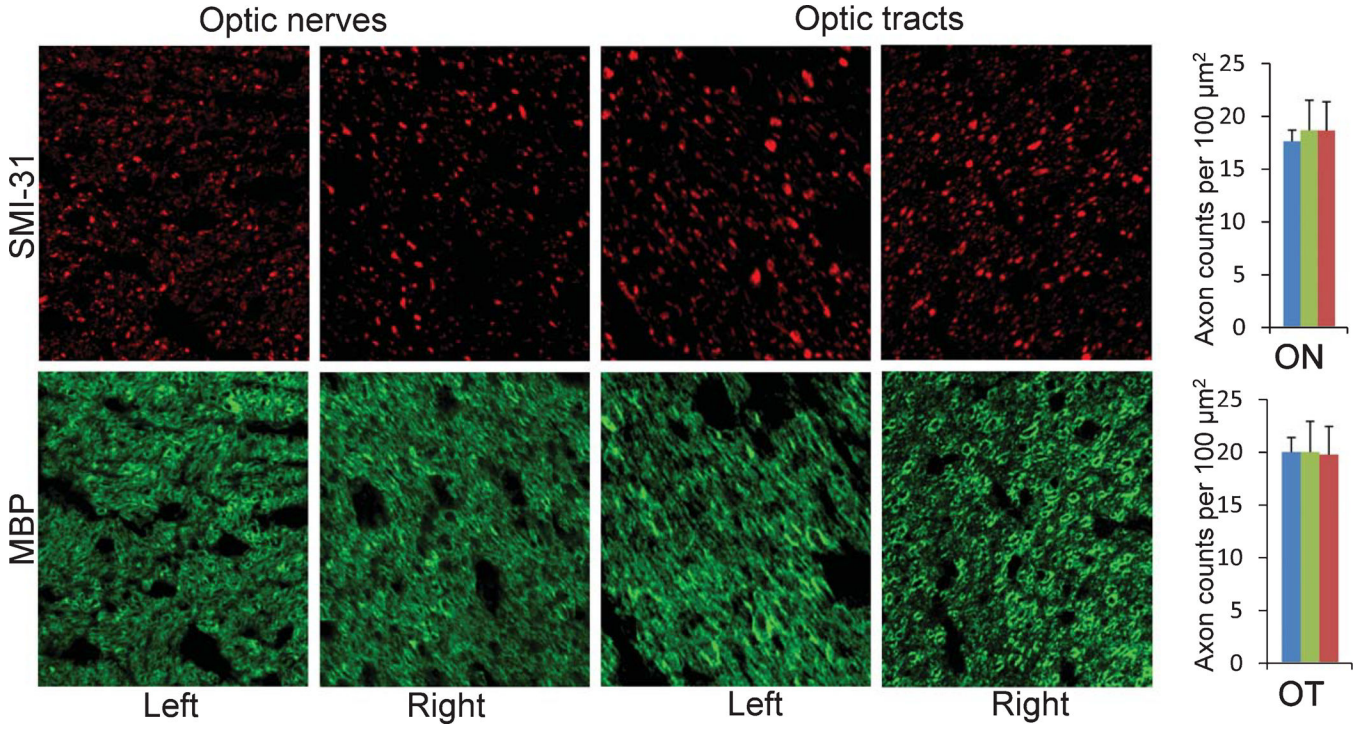

Fig. 3.

Immunohistochemistry (SMI-31 and MBP) of optic tracts and optic nerves of Aβ-treated mice. Because Aβ was injected in the left OT axonal terminal, left OT and right ON were expected to be directly affected by Aβ. However, both left and right ON and OT appeared no difference, compared to normal nerves. The bar graphs quantified the axonal numbers from left (green bars) and right (red bars) of ON and OT of Aβ-treated mice and normal mice (blue bars). The axonal counts showed no significant difference among these groups.

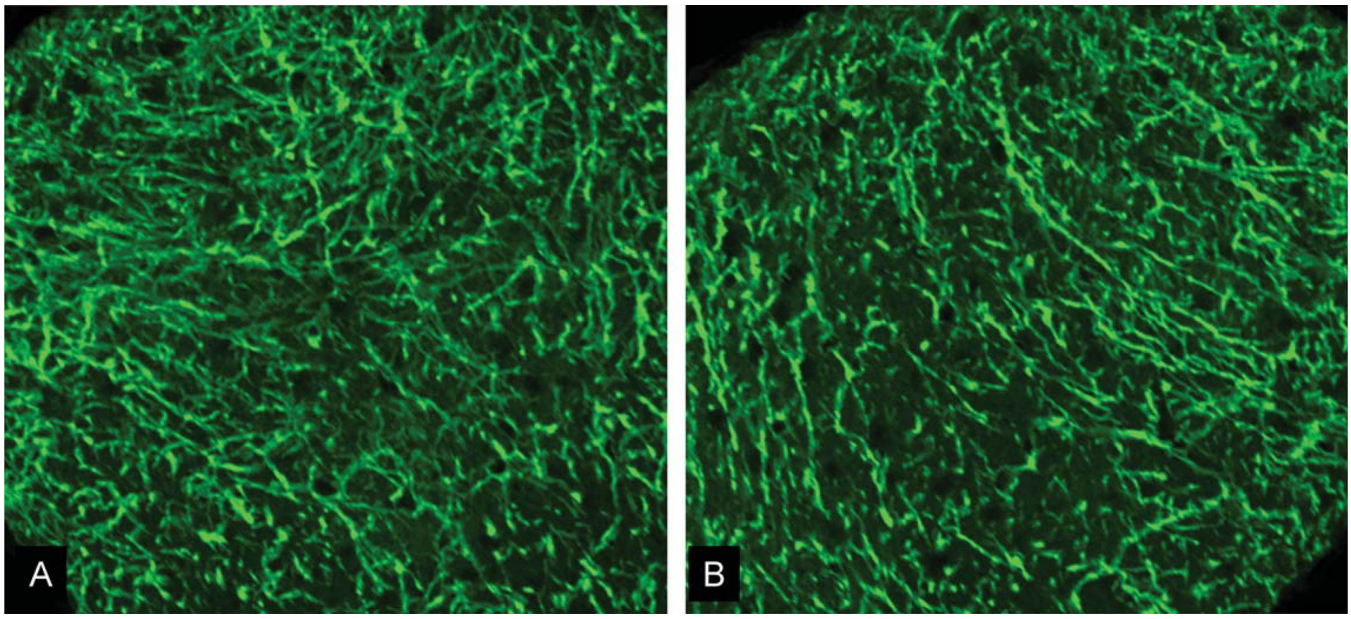

Fig. 4.

GFAP staining of the left (contralateral) and right (Aβ-affected) ON. Both showed normal morphology of astrocytes with no significant sign of injury.

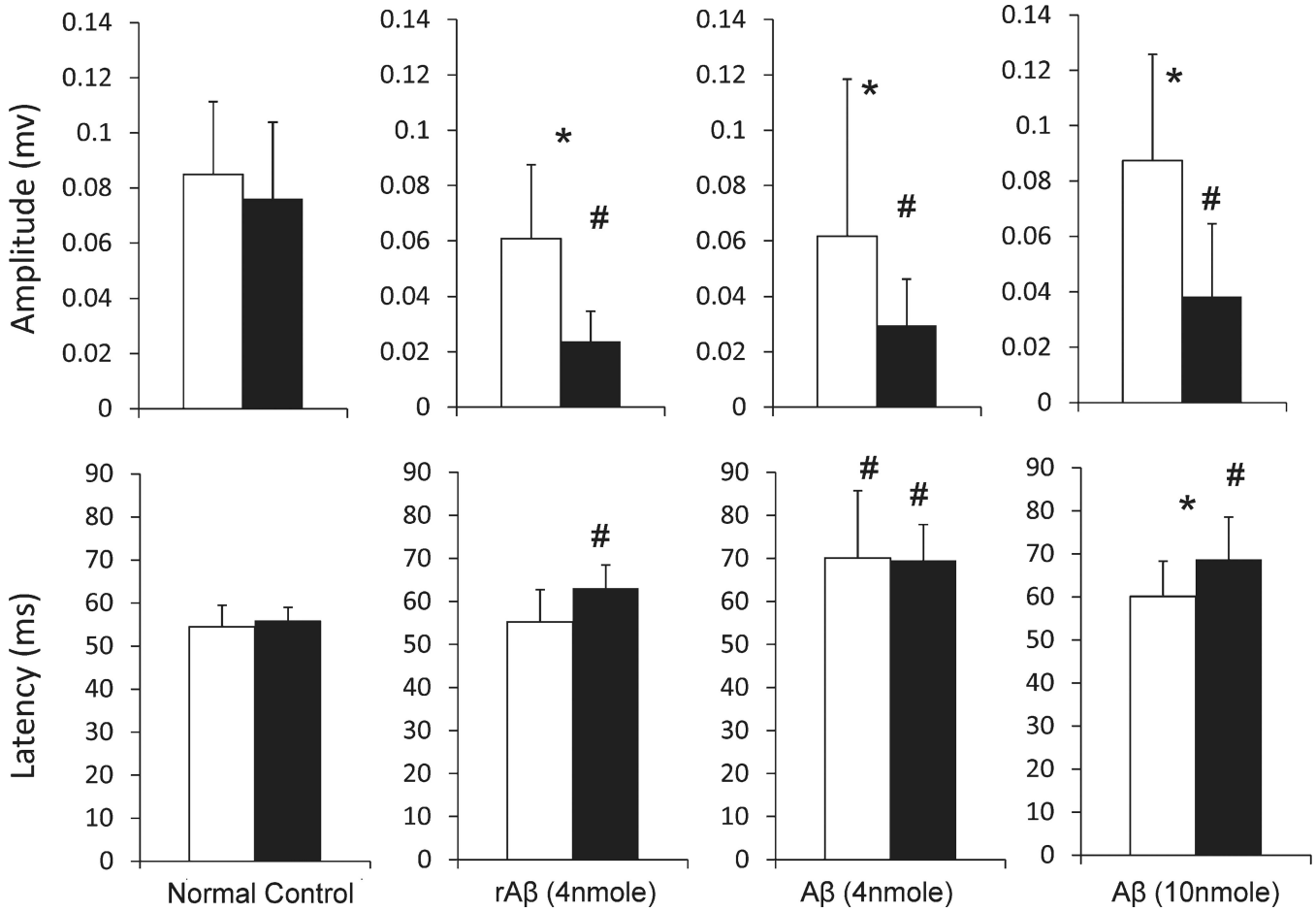

Fig. 5.

VEP amplitude and latency of left (white bars) and right eyes (black bars) of normal controls, and mice after Aβ and rAβ injection in the left side of OT axonal terminals. # and * indicates significant differences ($p < 0.05$) compared to the normal controls and between left and right, respectively.